

Metal-rich sludge from mine water treatment: from waste to effective arsenate adsorbent

Marco Tagliabue^{a,*}, Roberto Bagatin^a, Alessandro Conte^a, Annalisa Congiu^b,
Sara Perucchini^b, Stefano Zanardi^b, Michela Bellettato^c, Angela Carati^c

^aEni S.p.A., Renewable Energy and Environmental Laboratories, v. F. Maritano 26, I-20097, San Donato M.se, Italy,
emails: marco.tagliabue@eni.com (M. Tagliabue), roberto.bagatin@eni.com (R. Bagatin), alessandro.conte2@eni.com (A. Conte)

^bEni S.p.A., Renewable Energy and Environmental Laboratories, v. G. Fauser 4, I-28100, Novara, Italy,
email: annalisa.congiu@eni.com (A. Congiu), sara.perucchini@eni.com (S. Perucchini), stefano.zanardi@eni.com (S. Zanardi),

^cEni S.p.A., Downstream Process Technology Laboratories, v. F. Maritano 26, I-20097, San Donato M.se, Italy,
email: michela.bellettato@eni.com (M. Bellettato), angela.carati@eni.com (A. Carati)

Received 15 June 2016; Accepted 24 August 2016

ABSTRACT

Water contamination by arsenic is considered a global emergency due to both wide diffusion of this metalloid in the environment and its toxicity (10 µg/L arsenic concentration guideline value in drinking water has been recommended by World Health Organisation). This issue is dramatic in developing countries suffering of inadequate water treatment infrastructures. Within this framework, a great effort towards the development of economically viable technology for arsenic removal has been undertaken. In particular, adsorption on mining industry wastes has drawn attention due to the great affinity of arsenic oxy-anions for iron oxy-hydroxide. Opportunity of turning iron-rich sludge from an Italian mine-water treatment facility (underground pyrite deposits in Colline Metallifere district, Tuscany) into effective arsenic adsorbent was verified through laboratory-scale tests carried out in batch regime. Specifically, adsorption was considered as a polishing step assuming about 100 µg/L (i.e., 1.3 µmol/L) initial arsenic concentration as arsenate. Arsenic concentration below guideline value was obtained contacting the model solutions with 0.5 g/L adsorbent for 10 min with no appreciable interferences from competing anions (i.e., borate, hydrogen carbonate, phosphate, silicate and sulphate).

Keywords: Adsorption; Arsenate; Arsenic; Iron; Mine; Sludge; Water

1. Introduction

Arsenic is a metalloid exerting toxic effects in a variety of organisms including human beings. Chronic exposure to arsenicals has been correlated to important clinical manifestations including cancers (e.g., cancers of skin, lung and urinary bladder), cardiovascular disorders, diabetes and immune system alterations [1–3].

It is almost ubiquitous in the earth crust, and its mobilisation is an unavoidable process due to natural geo-chemical and biological cycling (e.g., geo-thermal activity, mineral weathering and assimilation by living organisms). On the other hand, environment contamination has been recently exacerbated by human activities connected to industry and agriculture (e.g., mineral mining, metal manufacturing and agro-chemicals diffusion).

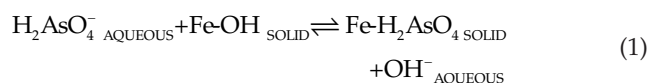
According to that, it has been estimated that about 10,000,000 people are at risk of exposing themselves

*Corresponding author.

Presented at the EDS conference on Desalination for the Environment: Clean Water and Energy, Rome, Italy, 22–26 May 2016.

to excessive arsenic levels with peaks in Argentina, Bangladesh, China, India, Mexico and Vietnam [1]. World Health Organisation (WHO) has recognised drinking water as one of the main route of exposure recommending a guideline concentration for arsenic of 10 µg/L [4]. This value has been acknowledged as a limit by most developed countries including members of European Union (EU) [5,6]. It is currently obtained by applying water treatment processes based on different operations: (i) precipitation (e.g., precipitation in presence of aluminium salts, iron salts and calcium hydroxide); (ii) membrane separation (e.g., reverse osmosis and electro-dialysis); and (iii) adsorption (e.g., adsorption on aluminium or iron oxide minerals and ion exchange on selective resins) [7,8]. Under neutral and oxidising conditions, arsenic is present in (V) oxidation state as arsenate (i.e., anions corresponding to the first and second dissociation of arsenic acid H_3AsO_4 with dissociation constants pK_{1-3} of 2.3, 6.8, 11.6, respectively). Conversely, under neutral and reducing conditions, arsenic is present in (III) oxidation state as arsenite (i.e., non-dissociated arsenous acid H_3AsO_3 with dissociation constants pK_{1-3} of 9.2, 12.1, 12.7, respectively) [3]. Experience has shown that arsenate removal is easier than arsenite. For this reason, raw water oxidation (e.g., aeration, chlorination, catalytic oxidation and photo-induced oxidation) is generally operated before arsenic removal [7–11].

Treatment processes based on adsorption have drawn great attention due to their intrinsic advantages: (i) simple operation; (ii) absence of continuously added reagents; (iii) infrastructure compactness; (iv) low labour cost; and (v) easy and safe handling of wastes. It has been estimated that about 80% of maintenance expenses has to be ascribed to adsorbent replacement that in turn depends on adsorbent cost [12]. For this reason, the development of cheap effective arsenic adsorbents is a way to further increase the competitiveness of adsorptive treatment process, especially in countries with limited access to funding. Adsorption on various oxide minerals containing iron in (III) oxidation state has been recognised as part of arsenic natural cycling and plenty of studies on this topic can be traced in literature [3,13–20]. Formation of monodentate and bidentate inner-sphere complexes involving surface hydroxyl groups has been inferred as a plausible complexation mechanism while segregation of iron arsenate has been excluded [21–24]. It can be sketched as reported in Eq. (1) [14]:



Taking inspiration from that, iron (III) oxy-hydroxide $FeO(OH)$ has found wide application as arsenic adsorbent due to its favourable characteristics including: (i) high arsenic oxy-anion capacity; (ii) acceptable selectivity towards different anions dissolved at concentration compatible with drinking water (e.g., borate, hydrogen carbonate, chloride, nitrate, phosphate, silicate and sulphate); (iii) high adsorption rate; (iv) acceptable performance over ranges of pH and ionic strength compatible with drinking water; (v) easy production; and (vi) safe disposal when exhausted [1–3,14,17,25,26]. Interestingly, various iron-rich wastes (e.g., residuals from water treatment, mineral mining and metal manufacturing) have been reported as valuable

raw materials for low-cost arsenic adsorbents preparation [17,18,27–36]. In spite of the promising results, comparison among various adsorbent performances remains difficult due to differences in reported composition, preparation and testing conditions. It makes experimental evaluation still a mandatory step to get realistic information.

This paper focuses on the opportunity of turning iron-rich sludge from an Italian mine-water treatment facility (underground pyrite deposits in Colline Metallifere district, Tuscany) into effective arsenic adsorbent adopting a minimal raw material work-up comprising drying, crushing and sieving operations. Approximately, effluent from inundated voids has been reported to have pH of 3.5 and concentrations of aluminium, iron (II), manganese (II) and sulphate of 50, 300, 10 and 2,500 mg/L, respectively. A typical oxidation-dosing-with-alkali-and-sedimentation treatment train has been implemented to comply with local regulations on water discharge in surface water bodies: (i) pH adjustment till about 8.5 by sodium hydroxide addition; (ii) iron (II) and manganese (II) oxidation to, respectively, iron (III) and manganese (IV) by hydrogen peroxide addition; (iii) flocculation and sedimentation of insoluble aluminium hydroxide $Al(OH)_3$, iron oxy-hydroxide $FeO(OH)$ and manganese dioxide MnO_2 in presence of cationic poly-acrylamide; (iv) sludge filtration and thickening through filter press; and (v) addition of calcium hydroxide to sludge and temporary storage before final disposal [37]. Laboratory-scale experimentation pointing to correlations among adsorbent performances (e.g., in term of specific capacity, selectivity and safety) and its physical-chemical characteristics was performed. Specifically, adsorption was considered as a polishing step assuming about 100 µg/L (i.e., 1.3 µmol/L) initial arsenic concentration as arsenate. Such experimental item allowed the determination of arsenic content as total arsenic by inductively coupled plasma (ICP) mass spectrometry [38,39].

2. Material and methods

2.1. Adsorbent, main reagents and laboratory equipment

Sludge samples (altogether about 3 kg) were taken from the mine water treatment facility just before their final disposal. They were further dried in laboratory at 20°C for 48 h under air flow, gently crushed in a mortar and sieved through calibrated stainless-steel screens mounted on a Retsch AS200 shaker. A powder with a particle size of less than 100 µm was recovered. The latter one was used as adsorbent for arsenic removal from water without further work-up.

Solutions were prepared adding reagent-grade solutes to deionised water got from a Millipore Milli-Q Gradient A10™ apparatus: di-sodium monohydrogen arsenate heptahydrate $Na_2HAsO_4 \cdot 7H_2O$ (Sigma-Aldrich), boric acid $B(OH)_3$ (Merck), sodium hydrogen carbonate $NaHCO_3$ (Carlo Erba), sodium hydroxide $NaOH$ (Carlo Erba), sodium nitrate $NaNO_3$ (Carlo Erba), nitric acid HNO_3 (Carlo Erba), sodium monohydrogen phosphate dodecahydrate $Na_2HPO_4 \cdot 12H_2O$ (VWR International), sodium silicate $(NaOH)_x \cdot (Na_2SiO_3)_y \cdot ZH_2O$ (27% wt/wt aqueous solution as SiO_2 , Sigma-Aldrich), and di-sodium sulphate Na_2SO_4 (Merck).

Tests were carried out at 20°C exploiting the laboratory temperature-conditioning system and using poly-propylene equipment rinsed with deionised water after overnight soaking into nitric acid 0.1 mol/L aqueous solution.

Solid-liquid separation was operated through 0.45 µm polytetrafluoroethylene syringe filters (CPS Analytica).

Solution pH was measured through a Hanna Instruments HI98103 Checker™.

Liquid samples were acidified till pH of 2.0 through few drops of reagent-grade nitric acid (Carlo Erba) and stored at 4°C until elemental analysis execution.

2.2. Physical-chemical characterisation

Elemental analysis was run by means of both X-ray fluorescence (XRF) spectroscopy and ICP methods depending on specific element: (i) XRF was employed for sulphur and silicon determination; (ii) ICP optical emission spectrometry ICP-OES (Thermo iCAP 6300 Duo™) was employed for determination of other main elements (i.e., other elements present at wt/wt % level); (iii) ICP mass spectrometry (ICP-MS; PerkinElmer, Elan DRC-e™) equipped with a dynamic reaction cell (DRC) was employed for trace elements determination. ICP methods on solids were conducted on dried at 20°C and digested samples. About 100 mg of adsorbent undergo complete mineralisation in a closed vessel device using temperature-controlled microwave heating with a mixture of [8 mL aqua-regia (hydrochloric acid/nitric acid at 3/1 v/v both Superpure RS™, Carlo Erba) + 1 mL hydrofluoric acid (Superpure RS™, Carlo Erba)]. External calibration was employed for all ICP methods (relative standard deviation [RSD] of 3%). Arsenic and lead quantifications were performed with ICP-MS using indium as internal standard. In particular, arsenic was monitored as AsO at mass 91 Da with oxygen as reaction gas (99.95% v/v, Rivoira). Wavelength-dispersive XRF spectroscopy (WD-XRF) was performed with a PANalytical Axios Advanced™ spectrometer equipped with a 4-kW rhodium anode X-ray tube, using WROXI™ standards (i.e., mixed oxides by British Geological Survey) and the fundamental parameters (FP) algorithm of the SuperQ™ software package. Solid samples were prepared as fused beads with a PANalytical Eagon2™ furnace fusion system. The K α radiations were employed for sulphur (2.308 keV) and silicon (1.740 keV) quantification (RSD of 10%).

Structural analysis was run through X-ray powder diffraction (XRD). It was carried out using a Philips X'Pert™ diffractometer equipped with a pulse-height analyser and a secondary monochromator. Data were collected in the 2 θ angular range from 3° to 80° with 0.03° 2 θ step and 20 s/step accumulation time. The CuK α radiation with wavelength of 1.54178 Å was used. Qualitative analysis was performed with a search-match method developed in the PANalytical X'Pert High Score™ software package.

Thermal analysis (i.e., thermogravimetric analysis and differential thermogravimetric analysis) was run through a Seiko TG/DTA6300™ thermobalance. About 13 mg of adsorbent were placed in an alumina crucible and heated under a 50-NmL/min air flow from 25°C to 950°C with a heating rate of 10°C/min at atmospheric pressure.

Total organic carbon (TOC) was determined through a Hach Lange TOC IL550™ instrument. About 70 mg of adsorbent were placed in an alumina crucible, digested

with reagent-grade hydrochloric acid (Carlo Erba), dried at 20°C and finally heated at 1,250°C under a 2,200-NmL/min oxygen flow (99.95% v/v, Rivoira) at atmospheric pressure. Minimum quantifiable limit (MQL) was about 130 µg/Kg.

Textural analysis was carried out from nitrogen (99.999% v/v, Air Liquide) adsorption-desorption isotherm curve acquired at -196°C by using a Micromeritics TriStar™ surface area and porosity analyser based on static-volumetric approach. About 0.4 g samples were used. Outgassing was operated at 100°C for 16 h applying rotary pump vacuum. Apparent specific surface area (A-SSA) in m²/g (Brunauer-Emmett-Teller method), specific pore volume V_p in mL/g (Gurvitch rule) and mean pore size d_p in Å (Barrett-Joyner-and Halenda method) were evaluated from acquired isotherm curve [40,41].

Point of zero charge (pH_{PZC}) was determined according to the mass titration method reported in [42]. Specifically, increasing amounts of adsorbent S as wt/wt % were mixed into different 50-mL sealable bottles each one containing 50 mL of 0.1 mol/L sodium nitrate aqueous solution set at pH of 10.5 by sodium hydroxide addition. Sodium nitrate was adopted as background electrolyte also in arsenate adsorption tests described in section 2.3 according to reported moderate-to-scarce interfering effect of nitrate [15,19,20,43–45]. Each suspension was continuously shaken at 20°C for 24 h at 15 1/min through a Velp Scientifica Rotax 6.8™ shaker. Finally, each suspension underwent pH measurement. The pH_{PZC} was assumed as the pH of the suspension having the higher adsorbent content when the pH evolution with solid concentration is low.

Determination was repeated twice and average values have been reported.

It has to be recalled that when pH is below pH_{PZC} solid surface is positively charged favouring anion adsorption due to electro-static attraction. Conversely, when pH is above pH_{PZC} solid surface is negatively charged, and anion adsorption has to compete with electro-static repulsion.

2.3. Leaching test

Leaching test was carried out on fresh adsorbent in order to evaluate release of metals and metalloids at concentrations non-compatible with EU drinking water legislation [5,6] according to procedure reported in [46]. Specifically, about 4.5 g of adsorbent on dry basis (referred to weight loss at 100°C from thermal analysis) were mixed into a 50-mL sealable bottle containing 45 mL of deionised water saturated with carbon dioxide (99.998% v/v, Rivoira). Suspension was continuously shaken at 20°C for 24 h at 15 1/min through a Velp Scientifica Rotax 6.8™ shaker. Finally, suspension was filtered and obtained clear solution (i.e., the leachate) underwent elemental analysis and pH measurement.

Elemental analysis was run through ICP on ten-times-diluted samples. ICP-OES was employed for iron quantification (emission line at 2,395.62 Å). All the other elements were detected by ICP-MS with external calibration employing indium as internal standard. Arsenic and selenium were analysed using DRC, respectively, as AsO at mass 91 Da with pure oxygen as reaction gas (99.95% v/v, Rivoira) and at mass 80 Da with methane as reaction gas (99.95% v/v, Rivoira).

Test was repeated twice, and average values have been reported.

2.4. Adsorption tests

Adsorption kinetic tests were studied mixing a definite amount of adsorbent into 2 L beakers containing 2 L of [about 100 µg/L arsenic + 0.10 mol/L sodium nitrate] aqueous solution. Specifically, two different tests were carried out with about 0.05 and 0.5 mg/L of adsorbent, respectively. Suspension was continuously stirred at 20°C for 24 h through an Ika C-MAG HS10™ magnetic stirrer. About 10 mL suspension aliquots were filtered at increasing contact times (i.e., at 5 min, every 10 min for the first hour, every hour for the following 5 h and finally after 24 h), and obtained clear solution samples underwent elemental analysis and pH measurement.

Adsorption equilibrium was evaluated through adsorption isotherm curve obtained mixing increasing amounts of adsorbent into different 1 L sealable bottles each containing 1 L of [about 100 µg/L arsenic + 0.10 mol/L sodium nitrate] aqueous solution. Specifically, six different tests were carried out with about 0.01, 0.05, 0.075, 0.1, 0.25, and 0.5 mg/L of adsorbent, respectively. Each suspension was continuously shaken at 20°C for 24 h at 15 1/min through a Velp Scientifica Rotax 6.8™ shaker. Finally, each suspension was filtered and obtained clear solution underwent elemental analysis as described in section 2.2 and equilibrium pH measurement.

Tests with 0.5 mg/L of adsorbents were repeated also in presence of competing anions considered one-at-a-time at concentrations compatible with EU drinking water legislation [5,6]: about 1 mg/L of boron (from boric acid), 2,500 mg/L of hydrogen carbonate, 1 mg/L of phosphate, 10 mg/L of silica (from sodium silicate), and 20 mg/L of sulphate, respectively.

Clear solution elemental analysis entailed both arsenic and iron quantification. The latter one was implemented as microfiltration effectiveness check assuming complete dissolution of any iron (III) oxy-hydroxide (i.e., the main adsorbent component) passing the filter after liquid sample acidification till pH of 2.0 as described in section 2.1.

No pH buffer was added in order to simulate conditions consistent with the simplest possible treatment and to follow pH evolution during adsorption.

Tests were repeated twice, and average values have been reported.

3. Results and discussion

Data from adsorbent elemental analysis collected in Table 1 point to aluminium (4.2 wt/wt %), calcium (9.3 wt/wt %), iron (24.3 wt/wt %) and magnesium (3.4 wt/wt %) as the main metals.

XRD pattern is reported in Fig. 1. Sharp reflections are related to calcite. No other crystalline phases are detected. Broad signals at 2θ of about 34° and 62° are consistent with the presence of poorly crystalline ferrihydrite according to [47,48]. Extremely fine dispersed iron oxides or hydroxides cannot be excluded (i.e., not indexed reflection at 2θ of about 23°). The same evidence result from adsorbent samples dried at higher temperatures till 100°C (data not reported).

Combined thermal profiles reported in Fig. 2 show a significant weight loss below 400°C, which reasonably corresponds to release of adsorbed water (i.e., maximum

Table 1
Fresh adsorbent chemical composition and surface characteristics

Parameter	Value
Al, % wt/wt	4.2
Ca, % wt/wt	9.3
Cu, % wt/wt	0.46
Fe, % wt/wt	24.3
Mg, % wt/wt	3.4
Mn, % wt/wt	0.78
Na, % wt/wt	0.45
Si, % wt/wt	1.4
S, % wt/wt	1.4
Zn, % wt/wt	0.92
As, mg/kg	157
Pb, mg/kg	192
A-SSA, m ² /g	226
V_p , mL/g	0.30
d_p , Å	160
pH _{PZC}	8.2

Note: A-SSA = apparent specific surface area; V_p = specific pore volume; d_p = pore size; pH_{PZC} = point of zero charge.

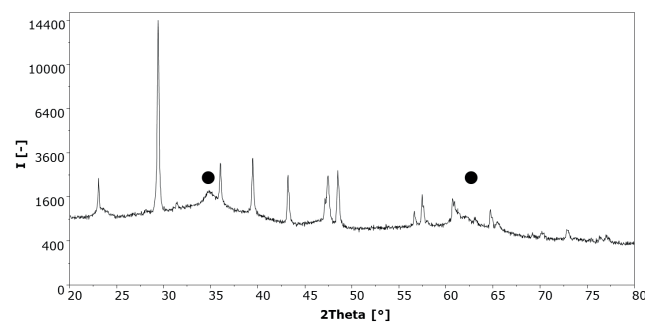


Fig. 1. Adsorbent XRD powder diffraction pattern: I = intensity; $[-]$ = intensity arbitrary units. Broad signals at 2θ of about 34° and 62° (both ones pointed by black circles) are consistent with the presence of poorly crystalline ferrihydrite according to [47,48].

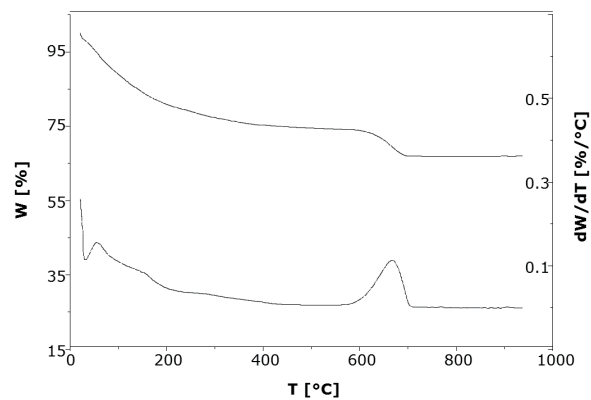


Fig. 2. Adsorbent combined thermal profiles: T = temperature; W = actual sample weight referred to initial one (top profile); dW/dT = sample weight variation with temperature as derivative (bottom profile).

at about 57°C in the derivative-weight curve) and of crystallisation water. Thermal decomposition of calcite can be observed starting from 550°C. The TOC is below MQL pointing to virtual absence of organics.

Adsorbent textural and surface characteristics are resumed in Fig. 3 and Table 1 as well.

In particular, adsorbent shows a Type IV nitrogen adsorption-desorption isotherm curve with a Type H1 hysteresis as sketched in Fig. 3. This behaviour is generally referred to mesoporous solids made by aggregates or agglomerates of spheroidal particles [40]. Further elaboration points to an A-SSA of 226 m²/g. These features resembles those traceable for other arsenic adsorbents based on iron (III) oxy-hydroxide [13,14,19,32,33,35,44,47,49].

Data reported in Fig. 4 and Table 2 indicate a p*H*_{PZC} charge of 8.2 within the range of values referred for various kind of aluminium hydroxide and iron (III) oxy-hydroxide [50]. It means that arsenate removal has to be preferably operated at pH below this value where adsorbent surface is positively charged (e.g., due to presence of protonated hydroxyl groups OH₂⁺ [43]).

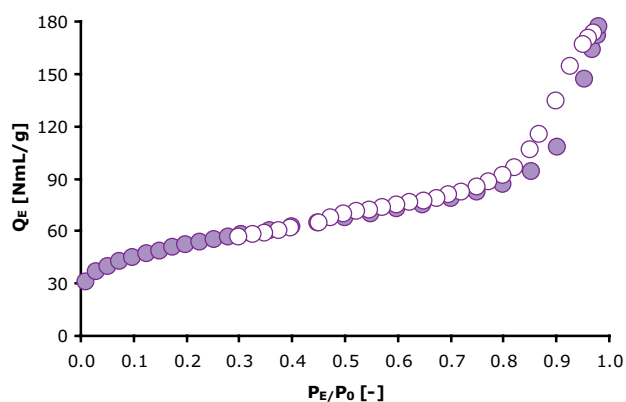


Fig. 3. Adsorbent nitrogen adsorption-desorption isotherm curve acquired at -196°C: filled circles = adsorption branch; open circles = desorption branch; P_E = actual nitrogen pressure at equilibrium; P_0 = nitrogen vapour pressure at -196°C; Q_E = specific capacity of adsorbed nitrogen at equilibrium [40,41].

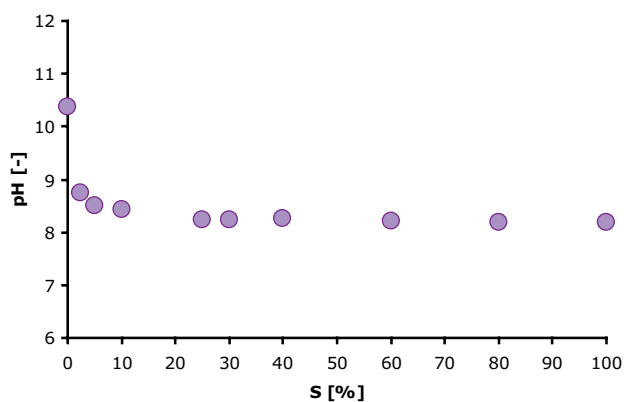


Fig. 4. Adsorbent mass titration curve acquired at 20°C: S = amount of adsorbent used to prepare suspension [42].

Results from leaching test reported in Table 3 notice aluminium concentration in leachate slightly higher than limit allowed by EU drinking water legislation. On the other hand, concentrations of other elements are acceptable. In particular, arsenic already present in fresh adsorbent (as evidenced in Table 1, probably from weathering of pyrite accompanying minerals) is virtually not released. This is a further evidence of the great affinity of arsenate (i.e., probably the most abundant arsenic form due to the oxidising environment promoted during mine water treatment) for iron (III) oxy-hydroxide.

Both kinetic tests resumed in Fig. 5 show quick decrease of arsenic concentration from 100 µg to less than 10 µg for contact time within 2 h. Afterwards, arsenic concentration tends to an asymptote assumed as equilibrium condition (data not reported for contact time higher than 5 h). Adsorption is faster in presence of the highest amount of adsorbent: acceptable arsenic concentrations are recorded after 10 min with 0.5 g/L adsorbent while 2 h are requested with 0.05 g/L. In both cases, after 24 h, the recovered clear solution is almost neutral and with less than 1.0 µg/L of arsenic and less than 30.0 µg/L of iron. The latter evidence points to effectiveness of the microfiltration operation. Data follow a pseudo-second-order kinetic describable by the linear model reported as Eq. (2) [51]:

$$\frac{t}{Q} = \frac{1}{k * Q_E^2} + \frac{t}{Q_E} \quad (2)$$

where Q is the specific capacity of adsorbed arsenic in µg/g after a defined contact time t in min; Q_E is the specific capacity of adsorbed arsenic at equilibrium and k is the observed kinetic constant in g/µg*min. Q is calculated as the difference between initial arsenic concentration in solution C_i

Table 2

Results from leaching test carried out on fresh adsorbent according to the procedure reported in [46]: leachate chemical composition and comparison with limits allowed by EU drinking water legislation [5,6]

Parameter	Value	Limit
pH	8.8	6.5–9.5
Al, µg/L	220.5	200
As, µg/L	0.35	10
B, µg/L	<40	1,000
Cd, µg/L	<0.3	5.0
Cr, µg/L	4.3	50
Cu, µg/L	8	2,000
Fe, µg/L	<30	200
Hg, µg/L	<0.8	1.0
Mn, µg/L	16.2	50
Ni, µg/L	4.6	20
Pb, µg/L	<0.7	10
Sb, µg/L	0.79	5.0
Se, µg/L	<0.4	10
Zn, µg/L	<30	5,000

Table 3

Arsenic removal efficiency η in presence of competing element J anions considered one-at-a-time at concentrations compatible with EU drinking water legislation [5,6]: about 1 mg/L of boron (from boric acid), 2,500 mg/L of hydrogen carbonate, 1 mg/L of phosphate, 10 mg/L of silica (from sodium silicate), 20 mg/L of sulphate. Values of pH at equilibrium pH_E are reported as well. Arsenate source is shown for the test without competing ions

Z	Source	J/As (mol/mol)	η ($\mu\text{g}/\text{L}/\mu\text{g}/\text{L}$)	pH_E
None	$\text{Na}_2\text{HAsO}_4 \cdot 7\text{H}_2\text{O}$	0	1.00	7.5
B	H_3BO_3	68	0.99	6.9
C	NaHCO_3	30,829	0.94	9.5
P	$\text{Na}_2\text{HPO}_4 \cdot 12\text{H}_2\text{O}$	10	0.99	9.5
S	Na_2SO_4	162	0.99	8.6
Si	$(\text{NaOH})_x(\text{Na}_2\text{SiO}_3)_y \cdot \text{ZH}_2\text{O}$	125	0.98	8.7

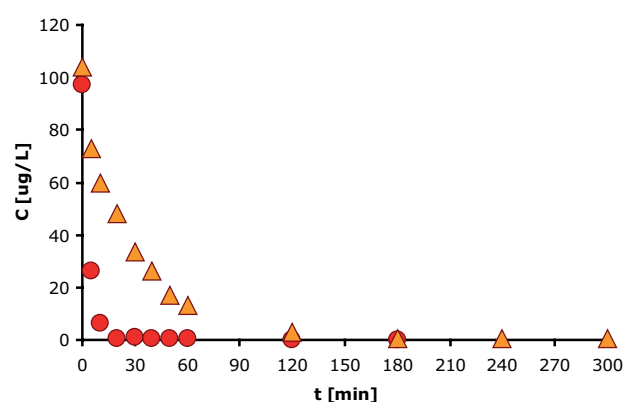


Fig. 5. Raw data referred to arsenic adsorption kinetic data acquired at 20°C: orange triangles = 0.05 g/L adsorbent; red circles = 0.5 g/L adsorbent; C = concentration of arsenic in solution at contact time t .

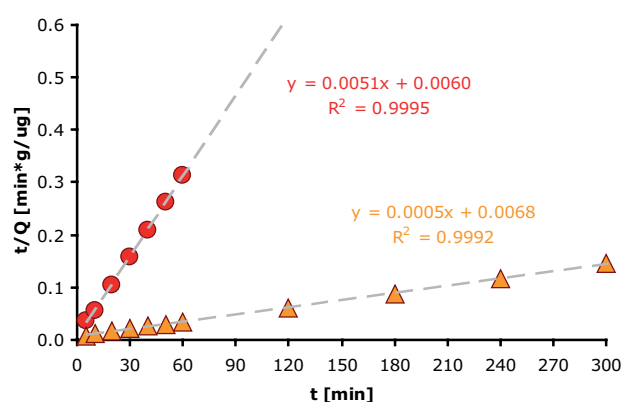


Fig. 6. Pseudo-second-order kinetic linear plot referred to arsenic adsorption kinetic data acquired at 20°C: orange triangles = 0.05 g/L adsorbent; red circles = 0.5 g/L adsorbent; Q = specific capacity of adsorbed arsenic at contact time t [51].

and those measured after a defined contact time C (both in $\mu\text{g}/\text{L}$) referred to the amount of added adsorbent M in g/L according to Eq. (3).

$$Q = \frac{(C_i - C)}{M} \quad (3)$$

Indeed, linear models represented in Fig. 6 show an excellent goodness of fit with correlation coefficients R^2 higher than 0.99. In both cases measured Q_E (i.e., 2,047 and 192 $\mu\text{g}/\text{g}$, respectively, for 0.05 and 0.5 g/L adsorbent) is close to Q_E computed from linear model slope (i.e., 2,000 and 196 $\mu\text{g}/\text{g}$, respectively, for 0.05 and 0.5 g/L adsorbent). Although these evidences agree with literature [35,51], any microkinetic hypotheses (out of the scope of this work) cannot be inferred without further experimentation.

Adsorption equilibrium is represented by the linear isotherm of Fig. 7. It can be interpreted assuming that adsorbent is far from saturation condition in the studied trace-level domain. The highest measured Q_E is 8,355 $\mu\text{g}/\text{g}$ (i.e., 8.4 mg/g). This value is within the range from about 0.6 to 42.9 mg/g reported for arsenic adsorbents based on iron (III) oxy-hydroxide. On the other hand, it has to be stressed that many published data refer to specific capacity of adsorbed arsenic at saturation conditions (i.e., the maximum obtainable value for each adsorbent at a defined temperature, often extrapolated from modelling) [36].

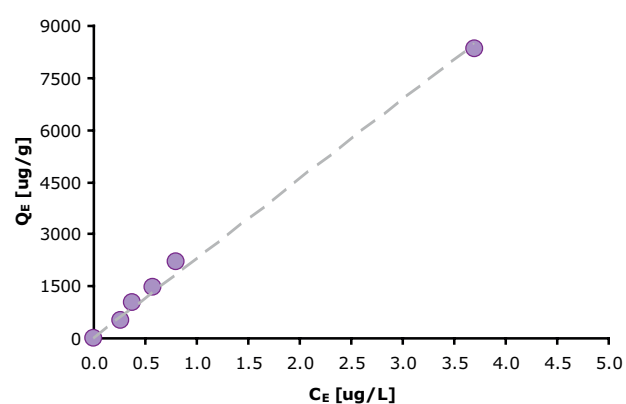


Fig. 7. Arsenic adsorption equilibrium data acquired at 20°C after 24 h: Q_E = specific capacity of adsorbed arsenic at equilibrium; C_E = concentration of arsenic in solution at equilibrium.

Values of arsenic removal efficiency η were computed according to Eq. (4) where C_i and C_E are initial and equilibrium arsenic concentration in solution, respectively. They are reported in Table 3 in order to quantify the effect of potentially interfering anions:

$$\eta = \frac{(C_I - C_E)}{C_I} \quad (4)$$

Literature points to phosphate as the most interfering anion due to the chemical analogy with arsenate while effects of borate, hydrogen carbonate, silicate, and sulphate are less pronounced or contradictory [20,28,43,45,49,52].

On the other hand, results collected in Table 3 point to a virtual invariance of η in spite of the large molal ratios among arsenic and the other elements J added as competing anions. It can be explained assuming that available adsorption sites are enough to allocate both arsenate and competing anions, due to the low concentration of the former ones. Interestingly, equilibrium pH measured after arsenate adsorption in presence of competing ions pH_E is higher than those got in presence of sole arsenate. It can be inferred that hydroxyl release according to Eq. (1) is mainly due to complexation with competing ions being the latter ones in large excess with respect to arsenate [43,53]. In fact, starting from about 1 $\mu\text{mol/L}$ dissolved arsenate and supposing a release of one hydroxyl for each arsenate, we finally have 1 $\mu\text{mol/L}$ dissolved hydroxyls corresponding to pH of 8.0. With the same assumption, in case of about 10 $\mu\text{mol/L}$ dissolved phosphate, we finally have pH of 9.0. These values are close to the measured ones (pH_E of 7.5 and 9.5, respectively) considering that accurate complexation stoichiometry is actually unknown. Adsorption of anions different to arsenate and phosphate is less efficient [20,28,43,45,49,52]: it could explain the limited increase of pH in the presence of larger concentrations of borate, hydrogen carbonate, silicate and sulphate. It has to be noticed that in most cases pH_E is slightly higher than measured adsorbent pH_{PZC} of 8.2. Under such conditions, adsorbent is slightly negatively charged and further arsenate adsorption could be hindered by electrostatic repulsion. It has also to be pointed out that increase of pH determines a speciation shift from di-hydrogen arsenate (prevailing till pH of about 7.0) to monohydrogen arsenate [3]. In spite of both described phenomena, no appreciable effect of pH on η can be traced in Table 3.

4. Conclusion

Sludge from mine water treatment facility has been turned into effective arsenate adsorbent based on poorly crystallised iron (III) oxy-hydroxide with minimal work-up. Several relevant features have been reported from laboratory-scale tests: (i) arsenic limit for drinking water can be got with minimal amounts of adsorbents in polishing tests; (ii) used adsorbent can be easily removed by microfiltration; (iii) virtually no interferences from competing anions at concentrations compatible with drinking water have been registered; and (iv) globally, data agree with those reported in literature.

On the other hand, several important questions remain open in view of a possible full-scale implementation. In particular, future activity has to consider: (i) arsenate adsorption tests till saturation for adsorbent evaluation in bulk removal operations; (ii) arsenite adsorption tests with identification of adsorbed species; (iii) identification of possible role of adsorbent minor composing elements

(e.g., manganese has been reported to promote oxidation of arsenite to arsenate [35,54]; (iv) adsorbent formulation in order to obtain pellets suitable for packed columns with minimal element release; (v) adsorbent tests under realistic conditions; and (vi) leaching tests on both fresh and used adsorbent under realistic conditions in order to evaluate adsorbent safety both during drinking water treatment and final disposal.

Acknowledgment

Ms. Monica Catrullo, Mr. Paolo Filtri and Mr. Massimo Nalli are acknowledged for their effective technical assistance.

References

- [1] J.C. Ng, J. Wang, A. Shraim, A global health problem caused by arsenic from natural sources, *Chemosphere*, 52 (2003) 1353–1359.
- [2] A.A. Duker, E.J.M. Carranza, M. Hale, Arsenic geochemistry and health, *Environ. Int.*, 31 (2005) 631–641.
- [3] V.K. Sharma, M. Sohn, Aquatic arsenic: toxicity, speciation, transformation and remediation, *Environ. Int.*, 35 (2009) 743–759.
- [4] World Health Organisation, Chemical Hazards in Drinking Water: Arsenic, #WHO/SDE/WSH/03.04/75/Rev/1, World Health Organisation, Geneva, Switzerland, 2011. Available from: http://www.who.int/water_sanitation_health/dwq/chemicals/arsenic.pdf (Accessed on March 24, 2016).
- [5] Council of the European Union, Council Directive on the Quality of Water Intended for Human Consumption, #98/83/EC, Council of the European Union, Brussels, Belgium, 1998. Available from: ec.europa.eu/environment/water/water-drink/legislation_en.html (Accessed on March 24, 2016).
- [6] S. Sorlini, F. Gialdini, C. Collivignarelli, Metal leaching in drinking water domestic distribution system: an Italian case study, *Int. J. Environ. Health Res.*, 24 (2014) 497–514.
- [7] E.O. Kartinen, C.J. Martin, An overview of arsenic removal processes, *Desalination*, 103 (1995) 79–88.
- [8] T.S.Y. Choong, T.G. Chua, Y. Robiah, F.L. Gregory Koay, I. Azni, Arsenic toxicity, health hazards and removal techniques from water: an overview, *Desalination*, 217 (2007) 139–166.
- [9] J. Gregor, Arsenic removal during conventional aluminium-based drinking water treatment, *Water Res.*, 35 (2001) 1659–1664.
- [10] M. Zaw, M.T. Emmett, Arsenic removal from water using advanced oxidation process, *Toxicol. Lett.*, 133 (2002) 113–118.
- [11] J.C.J. Gude, L.C. Rietveld, D. van Halem, Fate of low arsenic concentrations during full-scale aeration and rapid filtration, *Water Res.*, 88 (2016) 566–574.
- [12] L. Wang, A.S.C. Chen, Costs for Arsenic Removal Technologies for Small Water Systems: United States Environmental Protection Agency Arsenic Removal Technology Demonstration Program, #EPA/600/R-11/090, United States Environmental Protection Agency, Cincinnati, Ohio, 2011. Available from: clu-in.org/download/contaminantfocus/arsenic/Arsenic-costs-600-R-11-090.pdf (Accessed on March 24, 2016).
- [13] V. Lenoble, O. Bouras, V. Deluchat, B. Serpaud, J.C. Bollinger, Arsenic adsorption onto pillared clays and iron oxides, *J. Colloid Interface Sci.*, 255 (2002) 52–58.
- [14] K. Banerjee, G.L. Amy, M. Prevost, S. Nour, M. Jekel, P.M. Gallagher, C.D. Blumenschein, Kinetic and thermodynamic aspects of adsorption of arsenic onto granular ferric hydroxide (GFH), *Water Res.*, 42 (2008) 3371–3378.
- [15] Y. Mamidy Payany, C. Hurel, N. Marmier, M. Roméo, Arsenic adsorption onto hematite and goethite, *C. R. Chim.*, 12 (2009) 876–881.

- [16] Y. Mamidy Payany, C. Hurel, N. Marmier, M. Roméo, Arsenic (V) adsorption from aqueous solution onto goethite, hematite, magnetite and zero-valent iron: effects of pH, concentration and reversibility, *Desalination*, 281 (2011) 93–99.
- [17] D. Giles, M. Mohapatra, T.B. Issa, S. Anand, P. Singh, Iron and aluminium based adsorption strategies for removing arsenic from water, *J. Environ. Manage.*, 92 (2011) 3011–3022.
- [18] M. Gallegos Garcia, K. Ramirez Muniz, S. Song, Arsenic removal from water by adsorption using iron oxide minerals as adsorbents: a review, *Miner. Process. Extr. Metall. Rev.*, 33 (2012) 301–315.
- [19] T. Mahmood, S.U. Din, A. Naeem, S. Mustafa, M. Waseem, M. Hamayun, Adsorption of arsenate from aqueous solution on binary mixed oxide of iron and silicon, *Chem. Eng. J.*, 192 (2012) 90–98.
- [20] G. Yang, Y. Liu, S. Song, Competitive adsorption of arsenic (V) with co-existing ions on porous hematite in aqueous solutions, *J. Environ. Chem. Eng.*, 3 (2015) 1497–1503.
- [21] G.A. Waychunas, B.A. Rea, C.C. Fuller, J.A. Davis, Surface chemistry of ferrihydrite: Part 1. EXAFS studies of the geometry of co-precipitated and adsorbed arsenate, *Geochim. Cosmochim. Acta*, 57 (1993) 2251–2269.
- [22] C.C. Fuller, J.A. Davis, G.A. Waychunas, Surface chemistry of ferrihydrite: Part 2. Kinetics of arsenate adsorption and co-precipitation, *Geochim. Cosmochim. Acta*, 57 (1993) 2271–2282.
- [23] B. Manning, S.S.E. Fendorf, S. Goldberg, Surface structures and stability of arsenic (III) on goethite: spectroscopic evidences for inner-sphere complexes, *Environ. Sci. Technol.*, 32 (1998) 2383–2388.
- [24] S. Goldberg, C.T. Johnston, Mechanisms of arsenic adsorption on amorphous oxides evaluated using macroscopic measurements, vibrational spectroscopy and surface complexation modelling, *J. Colloid Interface Sci.*, 234 (2001) 204–216.
- [25] S. Tresintsi, K. Simeonidis, G. Vourlias, G. Stravapoulos, M. Mitrakas, Kilogram-scale synthesis of iron oxy-hydroxides with improved arsenic removal capacity: study of iron (II) oxidation-precipitation parameters, *Water Res.*, 46 (2012) 5255–5267.
- [26] M. Shafiquzzaman, M. Shafiul Azam, J. Nakajima, Q. Hamidul Bari, Arsenic leaching characteristics of the sludges from iron based removal process, *Desalination*, 261 (2010) 41–45.
- [27] H.S.A. Altundogan, S. Altundogan, F. Tuemen, M. Bildik, Arsenic adsorption from aqueous solutions by activated red mud, *Waste Manage.*, 22 (2002) 357–363.
- [28] H. Genc, J.C. Tjell, D. Mc Conchie, O. Schuiling, Adsorption of arsenate from water using neutralized red mud, *J. Colloid Interface Sci.*, 264 (2003) 327–334.
- [29] H. Genc, J.C. Tjell, D. Mc Conchie, Increasing the arsenate adsorption capacity of neutralized red mud (Bauxol™), *J. Colloid Interface Sci.*, 271 (2004) 313–320.
- [30] H. Genc, J.C. Tjell, D. Mc Conchie, Adsorption of arsenic from water using activated neutralized red mud, *Environ. Sci. Technol.*, 38 (2004) 3428–2434.
- [31] E. Tesser, E. D'Amato, R. Gori, C. Lubello, Conventional and innovative processes for neutral mine drainage treatment and reuse of residuals, Proc. of the 11th International Mine Water Association Congress, T.S. Ruede, A. Freund, C. Wolkersdorfer, Eds., Aachen, Germany, 2011, pp. 485–489. Available at: imwa.info/docs/imwa_2011/IMWA2011_Tesser_342.pdf (Accessed on March 24, 2016).
- [32] M.S. Ko, J.Y. Kim, J.S. Lee, J.I. Ko, K.W. Kim, Arsenic immobilisation in water and soil using acid mine drainage sludge, *Appl. Geochem.*, 35 (2013) 1–6.
- [33] K. Wu, R. Liu, T. Li, H. Liu, J. Peng, J. Qu, Removal of arsenic (III) from aqueous solution using a low-cost by-product in iron-removal plants-iron-based backwashing sludge, *Chem. Eng. J.*, 226 (2013) 393–401.
- [34] C. Trois, A. Cibati, South African sands as an alternative to zero valent iron for arsenic removal from an industrial effluent: batch experiments, *J. Environ. Chem. Eng.*, 3 (2015) 488–498.
- [35] D. Ocinski, I. Jacukowicz Sobala, P. Mazur, J. Raczek, E. Kociolek Balawieder, Water treatment residuals containing iron and manganese oxides for arsenic removal from water: characterisation of physical chemical properties and adsorption studies, *Chem. Eng. J.*, 294 (2016) 210–221.
- [36] M.K. Gibbons, G.A. Gagnon, Adsorption of arsenic from Nova Scotia groundwater onto water treatment residual solids, *Water Res.*, 44 (2010) 5740–5749.
- [37] P.L. Younger, S.A. Banwart, R.S. Hedin, *Mine Water: Hydrology, Pollution, Remediation*, Springer, Dordrecht, Holland, 2002, pp. 271–309.
- [38] K.A. Francesconi, D. Kuehnelt, Determination of arsenic species: a critical review of methods and applications, 2000–2003, *Analyst*, 129 (2004) 373–395.
- [39] S. D'Ilio, N. Violante, C. Majorani, F. Petrucci, Dynamic reaction cell inductively coupled plasma mass spectrometry for determination of total Ar, Cr, Se and V in complex matrices: still a challenge? A review, *Anal. Chi. Acta*, 698 (2011) 6–13.
- [40] G. Leofanti, M. Padovan, G. Tozzola, B. Venturelli, Surface area and pore texture of catalysts, *Catal. Today*, 41 (1998) 207–219.
- [41] M. Thommes, K. Kaneko, A.V. Neimark, J.P. Olivier, F. Rodriguez Reinoso, J. Rouquerol, K.S.W. Sing, Physisorption of gases, with special reference to the evaluation of surface area and pore size distribution, *Pure Appl. Chem.*, 87 (2015) 1051–1069.
- [42] J.P. Reymond, F. Kolenda, Estimation of the point of zero charge of simple and mixed oxides by mass titration, *Powder Technol.*, 103 (1999) 30–36.
- [43] J.B. Harrison, V.E. Berkheiser, Anion interactions with freshly prepared hydrous iron oxides, *Clays Clay Miner.*, 30 (1982) 97–102.
- [44] P.Y. Wu, Y. Jia, J.P. Jiang, Q.Y. Zhang, S.S. Zhou, F. Fang, Enhanced arsenate removal performance of nano-structured goethite with high content of surface hydroxyl groups, *J. Environ. Chem. Eng.*, 2 (2014) 2312–2320.
- [45] C. Su, R.W. Puls, Arsenate and arsenite removal by zerovalent iron: effects of phosphate, silicate, carbonate, borate, sulphate, chromate, molybdate and nitrate, relative to chloride, *Environ. Sci. Technol.*, 35 (2001) 4562–4568.
- [46] Ente Italiano di Normazione, Characterisation of Waste. Leaching. Compliance Test for Leaching of Granular Waste Materials and Sludges: Part 2. One Stage Batch Test at a Liquid to Solid Ratio of 10 L/kg for Materials with Particle Size below 4 mm (without or with Size Reduction), #UNI EN 12457-2:2004, Ente Italiano di Normazione, Milano, Italy, 2004. Available from: store.uni.com/magento-1.4.0.1/index.php/catalogsearch/result/?q=124572++2004&fulltext=fulltext&tpqual%5B3%5D=zz&tpqual_var=99&ttbloc=0# (Accessed on March 24, 2016).
- [47] S. Das, M.J. Hendry, J. Essilfie Dughan, Transformation of two-line ferrihydrite to goethite and hematite as a function of pH and temperature, *Environ. Sci. Technol.*, 45 (2011) 268–275.
- [48] V.A. Drits, B.A. Sakharov, A.L. Salyn, A. Manceau, Structural model for ferrihydrite, *Clay Miner.*, 28 (1993) 185–207.
- [49] P.J. Swedlund, J.G. Webster, Adsorption and polymerization of silicic acid on ferrihydrite and its effect on arsenic adsorption, *Water Res.*, 33 (1999) 3413–3422.
- [50] M. Kosmulski, pH-dependent surface charging and points of zero charge II. Update, *J. Colloid Interface Sci.*, 275 (2004) 214–224.
- [51] S.S. Gupta, K.G. Bhattacharyya, Kinetics of adsorption of metal ions on inorganic materials: a review, *Adv. Colloid Interface Sci.*, 162 (2011) 39–58.
- [52] X. Meng, S. Bang, G.P. Korfiatis, Effects of silicate, sulphate and carbonate on arsenic removal by ferric chloride, *Water Res.*, 34 (2000) 1255–1261.
- [53] A. Jain, K.P. Raven, R. Loeppert, Arsenite and arsenate adsorption on ferrihydrite: surface charge reduction and net OH⁻ release stoichiometry, *Environ. Sci. Technol.*, 33 (1999) 1179–1184.
- [54] D.M. Singer, P.M. Fox, H. Guo, M.A. Marcus, J.A. Davis, Sorption and redox reactions of arsenic (III) and arsenic (V) within secondary mineral coatings on aquifer sediment grains, *Environ. Sci. Technol.*, 47 (2013) 11569–11576.